Current Biology, Vol. 12, 1157–1163, July 9, 2002, ©2002 Elsevier Science Ltd. All rights reserved. PII S0960-9822(02)00926-0

The Basic Helix-Loop-Helix Factor Olig2 Is Essential for the Development of Motoneuron and Oligodendrocyte Lineages

Hirohide Takebayashi,[1,5,6] Yoko Nabeshima,[1] Shosei Yoshida,[1] Osamu Chisaka,[2,3] Kazuhiro Ikenaka,[4] and Yo-ichi Nabeshima[1]

[1] Department of Pathology and Tumor Biology
Graduate School of Medicine
Kyoto University
Yoshida
Konoe-cho
Sakyo-ku
Kyoto 606-8501

[2] Faculty of Science

[3] Graduate School of Biostudies
Kyoto University
Kitashirakawa
Sakyo-ku
Kyoto 606-8502

[4] Laboratory of Neural Information
National Institute for Physiological Sciences
38 Nishigonaka
Myodaiji
Okazaki 444-8585
Japan

Summary

Sonic hedgehog (Shh), an organizing signal from ventral midline structures, is essential for the induction and maintenance of many ventral cell types in the embryonic neural tube. Olig1 and Olig2 are related basic helix-loop-helix factors induced by Shh in the ventral neural tube. Although expression analyses and gain-of–function experiments suggested that these factors were involved in motoneuron and oligodendrocyte development, they do not clearly define the functional differences between *Olig1* and *Olig2*. We generated mice with a homozygous inactivation of *Olig2*. These mice did not feed and died on the day of birth. In the spinal cord of the mutant mice, motoneurons are largely eliminated and oligodendrocytes are not produced. *Olig2*$^{-/-}$ neuroepithelial cells in the ventral spinal cord failed to differentiate into motoneurons or oligodendrocytes and expressed an astrocyte marker, S100β, at the time of oligodendrogenesis. Olig1 or Olig3, other family members, were expressed in the descendent cells that should have expressed Olig2. We concluded that Olig2 is an essential transcriptional regulator in motoneuron and oligodendrocyte development. Our data provide the first evidence that a single gene mutation leads to the loss of two cell types, motoneuron and oligodendrocyte.

[5] Correspondence: takebaya@lmls.med.kyoto-u.ac.jp

[6] Present address: Laboratory of Neural Information, National Institute for Physiological Sciences, 38 Nishigonaka, Myodaiji, Okazaki 444-8585, Japan.

Results and Discussion

Motoneuron and oligodendrocyte lineages are thought to be closely related by many lines of evidence [1]. They are sequentially generated in the ventral ventricular zone of the embryonic spinal cord during development. Lineage tracing experiments using retroviruses [2] or clonal culture of neuroepithelial cells [3] suggested a shared motoneuron/oligodendrocyte lineage. Furthermore, both lineages are induced by sonic hedgehog (Shh), a ventralizing secreted factor from the notochord and floor plate, within the same concentration range [4–7]. However, the molecular mechanisms underlying this motoneuron/oligodendrocyte switch have remained unclear until recently.

Olig1 and Olig2 were first identified as Shh-induced oligodendrocyte-specific basic helix-loop-helix (bHLH) transcription factors [8, 9]. *Olig3* was the third member of the Olig family to be isolated [10]. Many studies have established that motoneurons [10–12] and oligodendrocyte progenitors [8, 9] are generated from the Olig2-expressing pMN domain. Interestingly, a neurogenic bHLH factor, Neurogenin2, is coexpressed with Olig2 at the time of motoneuron generation and is downregulated at the onset of oligodendrogenesis [11–13]. During this time, the pattern of Olig2 and Nkx2.2 expression switches from mutually exclusive to overlapping [13–15]. Consistent with this observation, combinatorial expression of transcription factors, Olig2/Neurogenin2 and Olig2/Nkx2.2, is sufficient to trigger the differentiation programs of motoneurons [11, 12] and oligodendrocytes [13, 14], respectively, in the chick embryonic neural tube. In the spinal cord, however, *Olig1* expression, and that of *Olig2*, is mostly overlapping, and thus gain-of-function experiments do not clearly define the functional differences between *Olig1* and *Olig2*. In this study, we analyzed the consequences of *Olig2* loss-of-function. We focused on *Olig2* to try to avoid redundancy, as *Olig2* expression in the early spinal cord is higher than that of *Olig1* [8–10], and *Olig2* has a broader expression domain in the embryonic forebrain [10, 16, 17].

To create a targeted disruption in *Olig2*, we replaced a fragment encoding *Olig2* with one encoding tamoxifen-inducible Cre recombinase, *CreER*^{TM} (Figure 1A) [18, 19]. Because we were able to easily distinguish CreER^{TM}-expressing cells due to CreER^{TM}'s cytoplasmic localization in the absence of tamoxifen, *CreER*^{TM} could be used as an expression marker in this study and was expressed under the control of the *Olig2* promoter. The deletion was confirmed by Southern blot analyses (Figures 1B and 1C). *Olig2*$^{+/-}$ mice showed no gross morphological abnormalities and were viable and fertile. In contrast, *Olig2*$^{-/-}$ mice did not feed and died on the day of birth (Figures 2A and 2B). The dead *Olig2*$^{-/-}$ pups seemed to lack tonicity in extension muscles and retained their in utero posture after delivery (Figure 2B).

In order to determine the cause of perinatal lethality, we analyzed spinal cord sections from E18.5 embryos. When the embryos were obtained by Caesarian section,

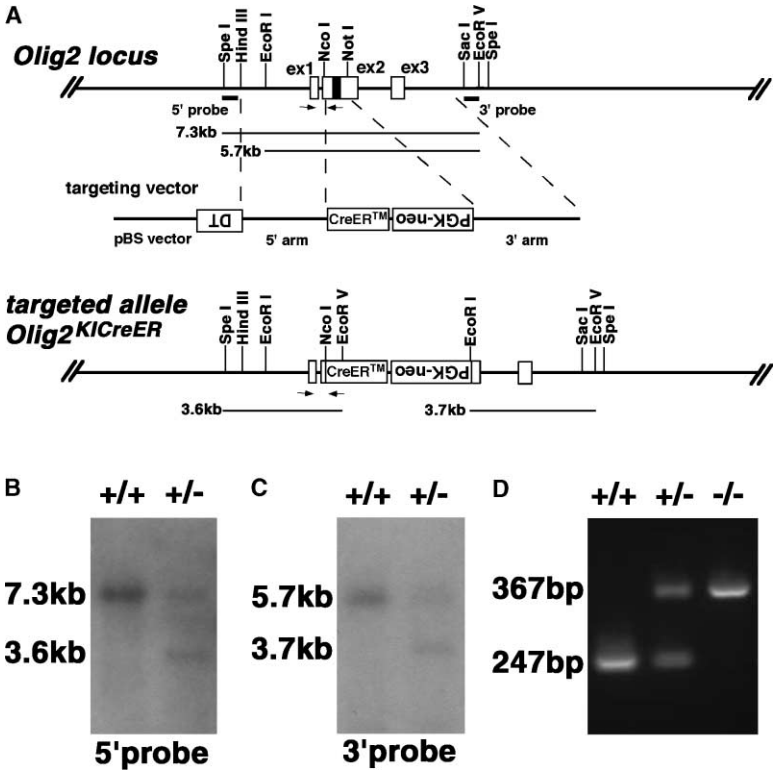

Figure 1. Targeted Mutation of the *Olig2* Locus

(A) Strategy for the targeted replacement of *Olig2* with tamoxifen-inducible Cre recombinase, *CreER*^{TM}. The filled box indicates the bHLH domain-encoding region. The open boxes indicate the exons. Exon 2 was replaced with *CreER*^{TM} and the PGK-neo cassette, and an EcoRV site was introduced. The 5′ and 3′ probes used for Southern blot analysis are shown below the wild-type genomic map. DT, diphteria toxin.

(B and C) Southern blot analyses of genomic DNA isolated from mouse tails. SpeI- and EcoRV-digested tail DNA was hybridized with a 5′ probe, and EcoRI- and EcoRV-digested tail DNA was hybridized with a 3′ probe. (B) The 5′ probe detects 7.3-kb wild-type and 3.6-kb mutant bands. (C) The 3′ probe detects 5.7-kb wild-type and 3.7-kb mutant bands.

(D) PCR analysis of tail DNA extracted from wild-type, *Olig2*$^{+/-}$, or *Olig2*$^{-/-}$ mice, using primers specific for the wild-type *Olig2* allele or the *Olig2*^{KICreER} allele. The positions of primers are shown in (A).

the *Olig2*$^{-/-}$ mice were easily distinguishable from their wild-type and *Olig2*$^{+/-}$ siblings by the gross morphology described above. Furthermore, the reflex movement of *Olig2*$^{-/-}$ mice to touching was uncoordinated, compared to their wild-type or *Olig2*$^{+/-}$ siblings, suggesting defect(s) in the neuronal circuits involved in spinal reflexes.

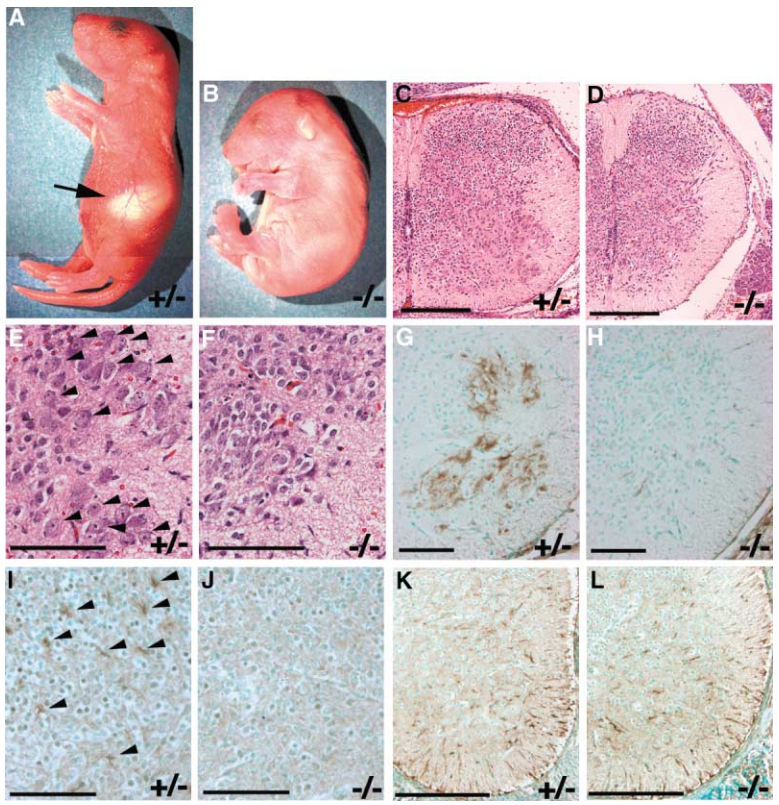

Figure 2. *Olig2*$^{-/-}$ Mice Have No Motoneurons and Oligodendrocytes in the Late Embryonic Spinal Cord

(A and B) Gross morphology of (A) *Olig2*$^{+/-}$ and (B) *Olig2*$^{-/-}$ newborn pups. The arrow in (A) indicates milk in the stomach. Note that the mutant mice have a shorter crown-rump length.

(C–F) Transverse sections of E18.5 spinal cords of (C and E) *Olig2*$^{+/-}$ and (D and F) *Olig2*$^{-/-}$ embryos stained by haematoxylin-eosin. The pictures in (E) and (F) show a higher magnification of the ventral horn depicted in (C) and (D). Note that the shape of the ventral horn in the knockout was altered (D) and that there are no motoneurons with big nuclei (F). The arrowheads in (E) indicate motoneurons in the ventral horn of the *Olig2*$^{+/-}$ mouse spinal cord.

(G and H) Neurofilament (NF) immunostaining of E18.5 spinal cords of (G) *Olig2*$^{+/-}$ and (H) *Olig2*$^{-/-}$ embryos. NF^{+} motoneurons are lost in the knockout.

(I and J) PDGFRα immunostaining of E18.5 spinal cords of (I) *Olig2*$^{+/-}$ and (J) *Olig2*$^{-/-}$ embryos. The arrowheads in (I) show PDGFRα^{+} oligodendrocyte progenitors in the dorsal spinal cord.

(K and L) GFAP immunostaining of E18.5 spinal cords of (K) *Olig2*$^{+/-}$ and (L) *Olig2*$^{-/-}$ embryos.

The scale bars in (C), (D), (K), and (L) represent 250 μm, and the scale bars in (E)–(J) represent 125 μm.

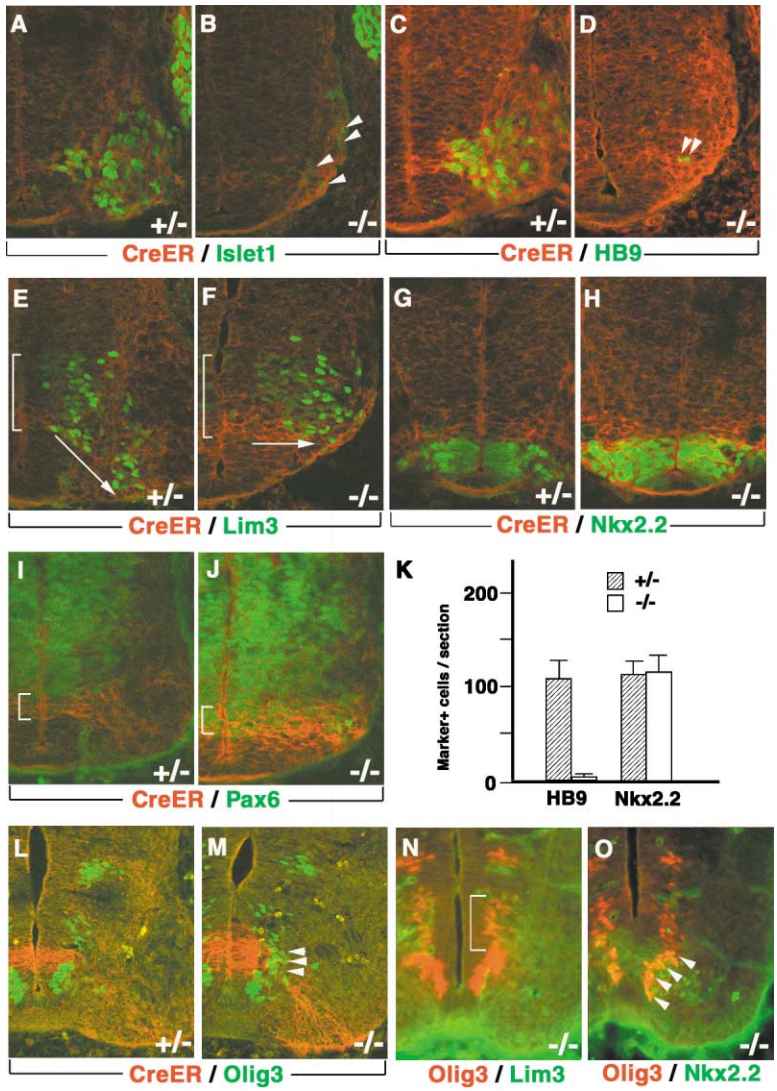

Figure 3. Loss of Motoneurons in the Early Embryonic Spinal Cord

(A–K) Double fluorescent immunohistochemistry was performed on transverse sections of the E10.5 thoracic spinal cord using combinations of the following antibodies. (A and B) Cre and Islet1, (C and D) Cre and HB9, (E and F) Cre and Lim3, (G and H) Cre and Nkx2.2, and (I and J) Cre and Pax6. The arrowheads in (B) and (D) indicate residual Islet1$^+$/HB9$^+$ motoneurons. Note that Islet1$^+$ D2 interneurons are also present in the dorsal part of the *Olig2*$^{-/-}$ spinal cord (data not shown) [41, 42]. The brackets in (E) and (F) show Lim3$^+$ cells producing domains p2 and pMN. The p2 domain, which gives rise to V2 interneurons, lies dorsal to the pMN domain. Note that Lim3$^+$ cells in the knockout migrate only in the lateral direction (arrow in [F]). The brackets in (I) and (J) show the CreER^{TM}-expressing pMN domain. Note that ventral expansion of Pax6 high expression into the pMN domain of the mutant was observed, in which there was normally lower Pax6 expression. Quantitative analysis is shown in (K). The number of marker positive cells is presented as the mean ± SD from six sections of two or three embryos. HB9$^+$ motoneurons decreased to <5%, while the number of Nkx2.2$^+$ V3 interneuron progenitors in the p3 domain did not change.

(L–O) Double fluorescent immunohistochemistry was performed on transverse sections of the E11.5 thoracic spinal cord using combinations of the following antibodies. (L and M) Cre and Olig3, (N) Olig3 and Lim3, and (O) Olig3 and Nkx2.2. Olig3 is normally expressed in the p0, p2, and p3 domains in the E11.5 spinal cord (L) [25], but the gap at pMN disappears in the mutant (M–O). The arrowheads in (M) show Olig3$^+$ cells in the pMN domain of the null mutant. The brackets in (N) show Olig3$^+$/Lim3$^+$ cells producing domains p2 and pMN. This results in the production of Olig3$^+$/Lim3$^+$ cells from the CreER^{TM}-expressing domain (M and N). The arrowheads in (O) show Olig3/Nkx2.2 double-positive cells.

Consistent with this observation, we found that there were no motoneurons in the ventral horn of the *Olig2*$^{-/-}$ spinal cord at any of the levels examined (Figures 2C–2F). This defect was also confirmed by neurofilament staining of motoneurons (Figure 2G and 2H). In addition to the loss of motoneurons, *Olig2*$^{-/-}$ mice had no oligodendrocyte progenitors that expressed platelet-derived growth factor α-receptor (PDGFRα) in the spinal cord (Figures 2I and 2J). We did not observe any obvious change in glial fibrillary acidic protein (GFAP) expression (Figures 2K and 2L). This result suggests that loss of Olig2 does not perturb the generic astrocyte differentiation program; however, we could not rule out a minor effect on the astrocyte subpopulation from the pMN domain (see below).

There are two possible explanations for the absence of motoneurons in *Olig2*$^{-/-}$ mice. One is that motoneurons are not generated, and the other is that motoneurons are produced but do not survive. We analyzed spinal cord sections from E10.5 mice and found only a few Islet1$^+$/HB9$^+$ motoneurons [20–23] in the *Olig2*$^{-/-}$ spinal cord (Figures 3A–3D and 3K). Interestingly, Lim3$^+$ cells were produced from both the p2 and pMN domains in the *Olig2*$^{-/-}$ spinal cord, as seen in that of *Olig2*$^{+/-}$, but the migration direction of Lim3$^+$ cells from the pMN domain was altered. In the mutant, Lim3$^+$ cells from the CreER^{TM}-expressing pMN domain migrated into the lateral margin of the cord like Lim3$^+$ cells from the p2 domain (Figures 3E and 3F, arrows). There were no obvious changes in the Nkx2.2-expressing p3 domain (Figures 3G, 3H, and 3K), but ventral expansion of Pax6 high expression into the pMN of the mutant was observed, in which there was normally lower Pax6 expression (Figures 4I and 4J, brackets) [24]. In the E11.5 ventral spinal cord, the CreER^{TM}-expressing neuroepithelial cells were extending radial fiber-like processes to ventral pia mater in both *Olig2*$^{+/-}$ and *Olig2*$^{-/-}$ spinal cords (Figures 3L and 3M). Olig3 was normally expressed in the lateral margin of the ventricular zone at the levels of p0, p2, and p3 (Figure 3L) [25]. However, the gap in Olig3 expression at the level of the pMN domain was absent in the null mice, with uninterrupted expression of Olig3 in

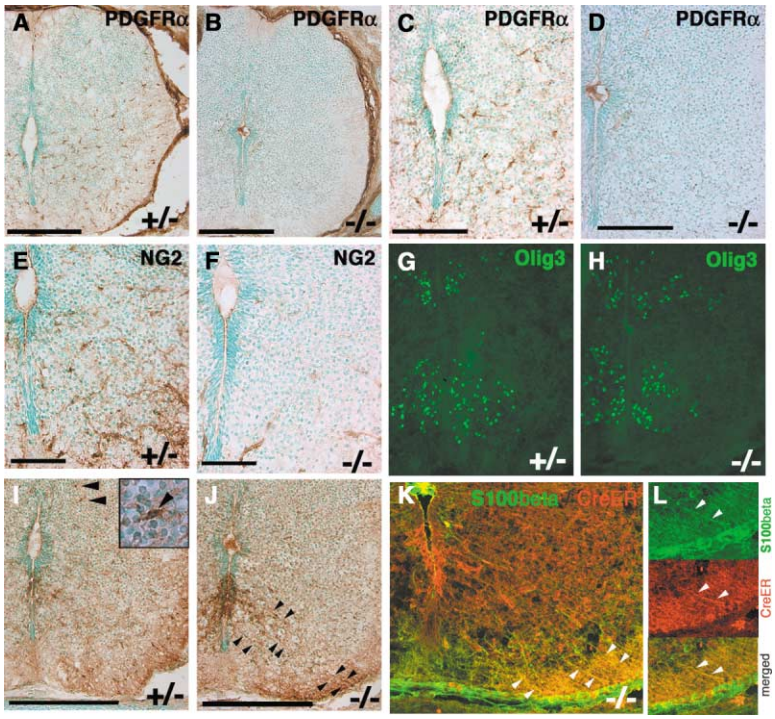

Figure 4. Oligodendrocytes Fail to Develop in the *Olig2*$^{-/-}$ Spinal Cord

(A–L) Sections of (A, C, E, G, and I) *Olig2*$^{+/-}$ and (B, D, F, H, J, K, and L) *Olig2*$^{-/-}$ spinal cords at E14.5 were subjected to immunohistochemistry with antibodies against (A–D) PDGFRα, (E and F) NG2, (G and H) Olig3, (I and J) Cre, and (K and L) Cre and S100β. There are no PDGFRα^{+} or NG2^{+} oligodendrocyte progenitors in the *Olig2*$^{-/-}$ spinal cord. In (E) and (F), the tube-like structures are background staining of blood vessels. (G and H) The expression of Olig3 was not dramatically altered in the *Olig2*$^{-/-}$ spinal cord (green nuclear staining). (I and J) Different morphology of CreER^{TM}-expressing cells in the *Olig2*$^{+/-}$ and *Olig2*$^{-/-}$ spinal cords. The arrowheads in (I) indicate oligodendrocyte progenitors migrating toward the dorsal spinal cord. The inset in (I) shows higher magnification of migrating oligodendrocyte progenitors. The arrowheads in (J) indicate radial fiber-like processes. (K and L) CreER^{TM}-expressing Olig2 null cells express an astrocyte marker, S100β. The arrowheads indicate S100β/CreER^{TM} double-positive radial processes. The scale bars in (A) and (B) represent 250 μm, and the scale bars in (C–F), (I), and (J) represent 125 μm.

the lateral margin of the ventricular zone from p2 to p3 (Figures 3M–3O). Therefore, ventral expansion of Olig3^{+}/Lim3^{+} cells, which are characteristic of immature V2 interneurons, was observed (Figure 3N). These data suggest that cells with molecular properties of V2 interneurons are produced in the CreER^{TM}-expressing Olig2 null domain and that Olig3 come to be expressed in the descendent cells that should have expressed Olig2. Olig3/Nkx2.2 double-positive cells were also observed in the p3 domain of the *Olig2*$^{-/-}$ spinal cord (Figure 3O, see below).

Next, we examined expression of oligodendrocyte progenitor markers, PDGFRα and NG2 proteoglycan [26], at E14.5, the time of oligodendrogenesis. Both markers are known to label oligodendrocyte progenitors, called O-2A progenitors [27, 28]. No PDGFRα^{+} or NG2^{+} oligodendrocyte progenitors were observed in the *Olig2*$^{-/-}$ spinal cord (Figures 4A–4F, 151 ± 15 [mean ± SD], PDGFRα^{+} cells/*Olig2*$^{+/-}$ section, 0 ± 0, PDGFRα^{+} cells/*Olig2*$^{-/-}$ section; at least 6 sections from 2–3 embryos). However, the expression of Olig3 was not dramatically altered in the mutant (Figures 4G and 4H). It has been proposed that two oligodendrocyte lineages exist in the embryonic spinal cord, one from pMN, the other from p3 [29, 13, 15]. Our results did not rule out the possibility that Nkx2.2^{+}/Olig1^{-}/Olig2^{-} oligodendrocytes from p3 are specified but fail to differentiate. Careful analysis of this second class of oligodendrocyte lineages is required, but there are no early specific markers for the lineage yet, and *Olig2* appears to be involved in the terminal differentiation step of both lineages [13, 15]. We investigated the cell fate of CreER^{TM}-expressing Olig2 null cells (Figures 4I–4L). In *Olig2*$^{+/-}$ mice, CreER^{TM}-expressing neuroepithelial cells lacked radial fiber like-processes, and migrating oligodendrocyte progenitors expressing CreER^{TM} were scattered even in the dorsal mantle zone (Figure 4I, inset and arrowheads). In *Olig2*$^{-/-}$ mice, CreER^{TM}-expressing cells still had radial fiber-like processes, which expressed an astrocyte marker, S100β [30], and never migrated to the dorsal spinal cord (Figures 4J–4L). These results suggest that the neuroepithelial cells failed to differentiate into oligodendrocyte progenitors and become astrocytes.

Previous studies have suggested that oligodendrocytes in the rostral regions of the neural tube also arise from the ventral central nervous system (CNS), similar to the situation seen in the spinal cord [31–33]. To look at the effect of the *Olig2* mutation on brain oligodendrocyte development, we examined PDGFRα expression in hindbrain/midbrain tissues at E18.5. In the mutant brain, very few PDGFRα^{+} cells were present (Figures 5A–5D). However, there were still Olig1-expressing cells in most regions of the CNS (Figure 5E, data not shown). Interestingly, there were also CreER^{TM}-expressing cells similarly distributed between *Olig2*$^{+/-}$ and *Olig2*$^{-/-}$ mice brains (Figure 5F, data not shown). These results indicate that Olig2 function is not necessary for the induction of Olig1 or the maintenance of Olig1/2 expression, and that Olig1 by itself is not sufficient to induce PDGFRα^{+} oligodendrocyte progenitors. Unexpectedly, we observed persisting PDGFRα^{+} cells in restricted areas of the *Olig2*$^{-/-}$ CNS such as the midbrain, diencephalon, cerebellum, and medulla (Figures 5G and 5H, data not shown). Zhou et al. and Lu et al. reported quite recently *Olig1/2* double-mutant mice and single knockout mice of *Olig1* and *Olig2*, respectively [34, 35]. Since no PDGFRα^{+} cells are observed in any brain areas of *Olig1/2* double mutants [34], they have shown that Olig1 function can compensate for the lack of Olig2 during oligodendrocyte development in the midbrain and hindbrain. Our previous

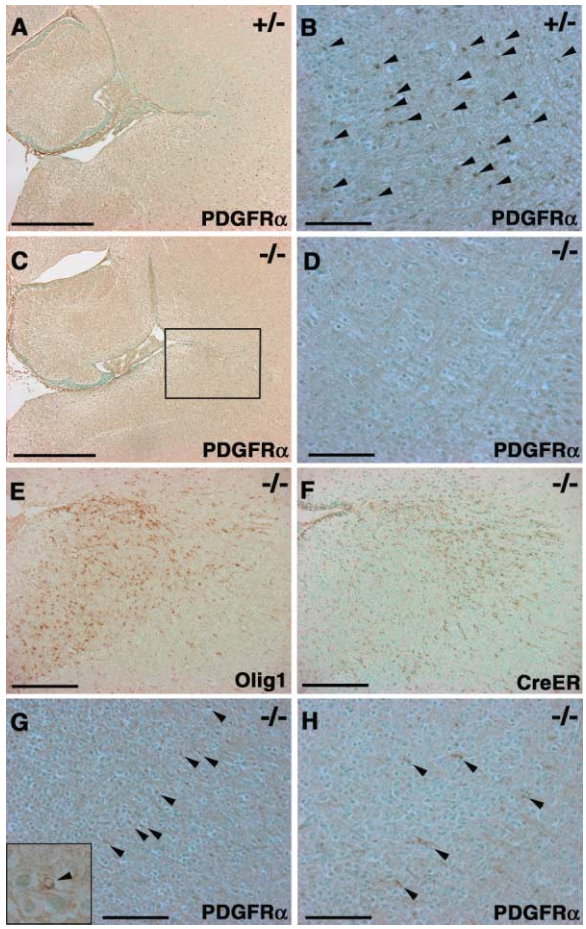

Figure 5. Defective Oligodendrocyte Differentiation in the *Olig2*$^{-/-}$ Brain

(A–H) Adjacent sagittal sections of E18.5 (A and B) *Olig2*$^{+/-}$ and (C–H) *Olig2*$^{-/-}$ brains were subjected to immunohistochemistry with antibodies against (A–D, G, and H) PDGFRα, (E) Olig1, or (F) ERα. The pictures in (B) and (D) show a higher magnification than that dipicted in (A) and (C). There were fewer PDGFRα$^+$ migrating oligodendrocyte progenitors than *Olig2*$^{+/-}$ in the hindbrain/midbrain region of the mutant mice (compare [A] and [B] and [C] and [D]). Note, however, there are still remaining PDGFRα$^+$ cells in restricted regions, such as the (G) superior colliculus and the (H) thalamus. The inset in (G) shows typical residual PDGFRα$^+$ cells with small nuclei and scarce cytoplasm. The arrowheads in (B), (G), and (H) indicate PDGFRα$^+$ cells. In spite of the decreased number of PDGFRα$^+$ oligodendrocyte progenitors, there were many Olig1- or CreER^{TM}-expressing cells in a similar distribution pattern (E and F). (E) and (F) show the high-power views corresponding to the black boxed area in (C). The scale bars in (A) and (C) represent 500 μm, the scale bars in (E) and (F) represent 250 μm, and the scale bars in (B), (D), (G), and (H) represent 125 μm.

gain-of-function experiments did not clearly define functional differences between *Olig1* and *Olig2*, that is, both combinations, Olig1/Neurogenin2 and Olig2/Neurogenin2, exhibited similar biological activity in terms of motoneuron generation [11]. Therefore, we assume that Olig1 can rescue Olig2 function if it is expressed in a large enough quantity at the proper time. However, we and others [35] observed that PDGFRα$^+$ cells persist only in restricted areas despite broad expression of Olig1. These observations raise an interesting possibility that related cofactor(s) other than Olig1 may also participate in the compensation for the loss of Olig2 function during oligodendrocyte development in the midbrain/hindbrain of *Olig2*$^{-/-}$ mice. It is notable that the oligodendrocyte lineage is proposed to originate from multiple restricted lineages based on early expression of proteolipid protein (PLP/DM20) and segregated expression between PDGFRα and PLP/DM20 [33, 36]. Interestingly, these Olig2-independent PDGFRα$^+$ cells were observed in the area (for example, medulla) in which the PLP/DM20-expressing oligodendrocyte lineage [36] or the PDGF-A-independent oligodendrocyte lineage [37] exist. What the relationship among these lineages is remains an unanswered question.

Long-term lineage-tracing experiments using tamoxifen-inducible Cre recombinase in this transgenic mouse model would provide us with a better understanding of the timing of the neuron/glia switch and the final fate of Olig2-expressing cells in normal or gene knockout contexts of development. Furthermore, we would be able to perform gene-activation or -inactivation experiments in specific cell lineages at specific developmental periods using tamoxifen treatment [19].

Experimental Procedures

Construction of the Targeting Vector

The *Olig2* BAC clone was obtained from a 129SVJ mouse BAC library by hybridization screening using a mouse *Olig2* cDNA probe (Incyte Genomics). We subcloned 3-kb HindIII-NcoI and 3.5-kb NotI-SacI fragments into a neo-resistance gene cassette vector. Most of the Olig2 ORF (aa 1–196) was deleted and replaced with *CreER*^{TM} using the NcoI site at the first methionine. CreER^{TM} is a tamoxifen-inducible form of Cre recombinase, which was made by fusing Cre recombinase and the ligand binding domain of the mutated estrogen receptor [38]. FLAG epitope was tagged to the C terminus of CreER^{TM}. The targeted allele is designated as *Olig2*^{KICreER}.

Electroporation and Generation of Germ Line-Transmitting Mice

TT2 ES cells (1×10^7) [39] were electoroporated with 50 μg linearized targeting vector DNA in 0.5 ml phosphate-buffered saline (PBS) using a Bio-Rad Gene Pulser. The electroporated cells were then cultured on feeder cells, which had been prepared from G418-resistant primary embryonic fibroblasts (GIBCO-BRL) and selected with G418 (300 μg/ml) for 6–8 days. Selected clones were cultured in a 96-well plate; the clones were then frozen, and their genomic DNA was isolated for Southern blot analysis.

Homologous recombinants, identified by Southern blot analysis using 5′ and 3′ external probes, were expanded for injection. Southern blot analyses of 656 ES cell clones identified two recombinants. Chimeric mice were generated by injection of the *Olig2* mutant ES cells into 8-cell-stage ICR embryos and were implanted into pseudopregnant foster mothers. The resulting chimeric males were bred with Balb/c females. The heterozygote mice were backcrossed with C57BL/6NCrj inbred mice.

Genotype Analysis

For PCR genotyping, the wild-type or targeted allele was detected using a common sense primer (5′-TCGAGAGCTTAGATCATCC-3′) and antisense primers specific for the wild-type *Olig2* (5′-CACCGC CGCCCAGTTTGTCC-3′) and *Olig2*^{KICreER} (5′-AGCATTGCTGTCACT TGGT-3′). These primer pairs amplify a 247-bp fragment from wild-type *Olig2* and a 367-bp fragment from *Olig2*^{KICreER}, respectively. PCR was performed at 95°C for 9 min, followed by 95°C for 20 s, 56°C for 30 s, and 72°C for 30 s; PCR was run for 37 cycles using Ampli Taq Gold (Roche).

Histology and Immunohistochemistry

Tissues were fixed with 4% PFA, paraffin-embedded, sectioned (4 μm), and stained with haematoxylin and eosin. For immunohistochemistry, 8 μm (paraffin) or 18 μm (cryo-) sections were made. Immunohistochemistry was performed as described [10]. Olig1 [11], Cre (Novagen), estrogen receptor (ER)α, PDGFRα (Santa Cruz), NG2 (kind gift of Dr. Joel Levine), and GFAP (DAKO) were detected using rabbit polyclonal antibodies (dilutions: anti-Olig1, 1/750; anti-Cre, 1/3000; anti-ERα, 1/150; anti-PDGFRα, 1/50; anti-NG2, 1/1000; and anti-GFAP, 1/2000). Olig3 [25] was detected using rat polyclonal antibody (1/500). PDGFRα (APA5, Pharmingen), S100β (SH-B1, Sigma), neurofilament [40], Nkx2.2, Pax6, Islet1, HB9, and Lim3 (DSHB) were detected using monoclonal antibodies (anti-PDGFRα, 1/500; anti-S100β, 1/1000; anti-neurofilament, 1/5; anti-Nkx2.2, 1/50; anti-Pax6, 1/20; anti-Islet1, 1/100; anti-HB9, 1/25; and anti-Lim3, 1/100). The rodent MNR2 homolog has not been identified, and the monoclonal antibody against MNR2 reacts with both MNR2 and HB9 in chicks. Since the staining pattern with the anti-chick MNR2 is very similar to the pattern that was previously reported with HB9 on the mouse tissue [22, 23], we used the anti-MNR2 antibody as the anti-HB9 antibody in this study.

Animals

For embryo staging, the day of detection of the vaginal plug was considered 0.5 dpc.

Acknowledgments

The authors wish to thank Dr. Trevor Littlewood for providing the mutated estrogen receptor clone, Dr. Joel Levine for anti-NG2 antibody, and Dr. Shenandoah Robinson for advice on rabbit polyclonal PDGFRα antibody staining. We are grateful to Mr. Makoto Okamura for constructing the *CreER*^{TM} fusion gene; Mr. Tsutomu Obata for making paraffin sections; Ms. Yoko Kurotaki for technical instruction in ES cell injection; Dr. Toshihiko Fujimori for discussion during the initial stage of this project; Dr. R.T. Yu for critical reading of the manuscript; and all members of the Ikenaka lab, especially Dr. Tetsushi Kagawa for helpful discussion, Dr. Noritaka Masahira for technical assistance, and Ms. Rie Taguchi for help in maintaining the mice colony. The monoclonal antibodies 2H3, 74.5A5, PAX6, 39.4D5, 81.5C10, and 67.4E12, developed by Drs. T.M. Jessell, J. Dodd, and A. Kawakami, were obtained from the Developmental Studies Hybridoma Bank maintained by the University of Iowa, Department of Biological Sciences. H.T. is a research fellow of the Japan Society for the Promotion of Science. This work was supported by research grants from the Japan Society for the Promotion of Science and the Ministry of Education, Science, Sports, and Culture of Japan.

Received: March 18, 2002
Revised: April 30, 2002
Accepted: May 16, 2002
Published: July 9, 2002

References

1. Richardson, W.D., Smith, H.K., Sun, T., Pringle, N.P., Hall, A., and Woodruff, R. (2000). Oligodendrocyte lineage and the motor neuron connection. Glia *29*, 136–142.
2. Leber, S.M., and Sanes, J.R. (1995). Migratory paths of neurons and glia in the embryonic chick spinal cord. J. Neurosci. *15*, 1236–1248.
3. Kalyani, A., Hobson, K., and Rao, M.S. (1997). Neuroepithelial stem cells from the embryonic spinal cord: isolation, characterization, and clonal analysis. Dev. Biol. *186*, 202–223.
4. Roelink, H., Augsburger, A., Heemskerk, J., Korzh, V., Norlin, S., Ruiz i Altaba, A., Tanabe, Y., Placzek, M., Edlund, T., Jessell, T.M., et al. (1994). Floor plate and motor neuron induction by vhh-1, a vertebrate homolog of hedgehog expressed by the notochord. Cell *76*, 761–775.
5. Pringle, N.P., Yu, W.P., Guthrie, S., Roelink, H., Lumsden, A., Peterson, A.C., and Richardson, W.D. (1996). Determination of neuroepithelial cell fate: induction of the oligodendrocyte lineage by ventral midline cells and sonic hedgehog. Dev. Biol. *177*, 30–42.
6. Poncet, C., Soula, C., Trousse, F., Kan, P., Hirsinger, E., Pourquie, O., Duprat, A.M., and Cochard, P. (1996). Induction of oligodendrocyte progenitors in the trunk neural tube by ventralizing signals: effects of notochord and floor plate grafts, and of sonic hedgehog. Mech. Dev. *60*, 13–32.
7. Orentas, D.M., Hayes, J.E., Dyer, K.L., and Miller, R.H. (1999). Sonic hedgehog signaling is required during the appearance of spinal cord oligodendrocyte precursors. Development *126*, 2419–2429.
8. Lu, Q.R., Yuk, D., Alberta, J.A., Zhu, Z., Pawlitzky, I., Chan, J., McMahon, A.P., Stiles, C.D., and Rowitch, D.H. (2000). Sonic hedgehog-regulated oligodendrocyte lineage genes encoding bHLH proteins in the mammalian central nervous system. Neuron *25*, 317–329.
9. Zhou, Q., Wang, S., and Anderson, D.J. (2000). Identification of a novel family of oligodendrocyte lineage-specific basic helix-loop-helix transcrition factors. Neuron *25*, 331–343.
10. Takebayashi, H. Yoshida, S., Sugimori, M., Kosako, H., Kominami, R., Nakafuku, M., and Nabeshima, Y. (2000). Dynamic expression of basic helix-loop-helix Olig family members: implication of Olig2 in neuron and oligodendrocyte differentiation and identification of a new member, Olig3. Mech. Dev. *99*, 143–148.
11. Mizuguchi, R., Sugimori, M., Takebayashi, H., Kosako, H., Nagao, M., Yoshida, S., Nabeshima, Y., Shimamura, K., and Nakafuku, M. (2001). Combinatorial roles of Olig2 and Neurogenin2 in the coordinated induction of pan-neuronal and subtype-specific properties of motor neurons. Neuron *31*, 757–771.
12. Novitch, B.G., Chen, A.I., and Jessell, T.M. (2001). Coordinate regulation of motor neuron subtype identity and pan-neuronal properties by the bHLH repressor Olig2. Neuron *31*, 773–789.
13. Zhou, Q., Choi, G., and Anderson, D.J. (2001). The bHLH transcription factor Olig2 promotes oligodendrocyte differentiation in combination with Nkx2.2. Neuron *31*, 791–807.
14. Sun, T., Echelard, Y., Lu, R., Yuk, D.I., Kaing, S., Stiles, C.D., and Rowitch, D.H. (2001). Olig bHLH proteins interact with homeodomain proteins to regulate cell fate acquisition in progenitors of the ventral neural tube. Curr. Biol. *11*, 1413–1420.
15. Fu, H., Qi, Y., Tan, M., Cai, J., Takebayashi, H., Nakafuku, M., Richardson, W.D., and Qiu, M. (2002). Dual origin of spinal oligodendrocyte progenitors and evidence for the cooperative role of Olig2 and Nkx2.2 in the control of oligodendrocyte differentiation. Development *129*, 681–693.
16. Nery, S., Wichterle, H., and Fishell, G. (2001). Sonic hedgehog contributes to oligodendrocyte specification in the mammalian forebrain. Development *128*, 527–540.
17. Tekki-Kessaris, N., Woodruff, R., Hall, A.C., Gaffield, W., Kimura, S., Stiles, C.D., Rowitch, D.H., and Richardson, W.D. (2001). Hedgehog-dependent oligodendrocyte lineage specification in the telencephalon. Development *128*, 2545–2554.
18. Brocard, J., Warot, X., Wendling, O., Messaddeq, N., Vonesch, J.L., Chambon, P., and Metzger, D. (1997). Spatio-temporally controlled site-specific somatic mutagenesis in the mouse. Proc. Natl. Acad. Sci. USA *94*, 14559–14563.
19. Danielian, P.S., Muccino, D., Rowitch, D.H., Michael, S.K., and McMahon, A.P. (1998). Modification of gene activity in mouse embryos in utero by a tamoxifen-inducible form of Cre recombinase. Curr. Biol. *8*, 1323–1326.
20. Ericson, J., Thor, S., Edlund, T., Jessell, T.M., and Yamada, T. (1992). Early stages of motor neuron differentiation revealed by expression of homeobox gene Islet-1. Science *256*, 1555–1560.
21. Pfaff, S.L., Mendelsohn, M., Stewart, C.L., Edlund, T., and Jessell, T.M. (1996). Requirement for LIM homeobox gene Isl1 in motor neuron generation reveals a motor neuron-dependent step in interneuron differentiation. Cell *84*, 309–320.
22. Tanabe, Y., William, C., and Jessell, T.M. (1998). Specification of motor neuron identity by the MNR2 homeodomain protein. Cell *95*, 67–80.
23. Arber, S., Han, B., Mendelsohn, M., Smith, M., Jessell, T.M., and Sockanathan, S. (1999). Requirement for the homeobox gene Hb9 in the consolidation of motor neuron identity. Neuron *23*, 659–674.

24. Ericson, J., Rashbass, P., Schedl, A., Brenner-Morton, S., Kawakami, A., van Heyningen, V., Jessell, T.M., and Briscoe, J. (1997). Pax6 controls progenitor cell identity and neuronal fate in response to graded Shh signaling. Cell *90*, 169–180.
25. Takebayashi, H., Ohtsuki, T., Uchida, T., Kawamoto, S., Okubo, K., Ikenaka, K., Takeichi, M., Chisaka, O., and Nabeshima, Y. (2002). Non-overlapping expression of Olig3 and Olig2 in the embryonic neural tube. Mech. Dev. *113*, 169–174.
26. Levine, J.M., and Stallcup, W.B. (1987). Plasticity of developing cerebellar cells in vitro studied with antibodies against NG2 antigen. J. Neurosci. *7*, 2721–2731.
27. Raff, M.C., Miller, R.H., and Noble, M. (1983). A glial progenitor cell that develops in vitro into an astrocyte or an oligodendrocyte depending on culture medium. Nature *303*, 390–396.
28. Nishiyama, A., Lin, X.H., Giese, N., Heldin, C.H., and Stallcup, W.B. (1996). Co-localization of NG2 proteoglycan and PDGF alpha-receptor on O2A progenitor cells in the developing rat brain. J. Neurosci. Res. *43*, 299–314.
29. Xu, X., Cai, J., Fui, F., Qi, Y., Modderman, G., Liu, R., and Qiu, M. (2000). Selective expression of Nkx-2.2 transcription factor in the migratory chicken oligodendrocyte progenitor cells and implications for the embryonic origin of oligodendrocytes. Mol. Cell. Neurosci. *16*, 740–753.
30. Ghandour, M.S., Langley, O.K., Labourdette, G., Vincendon, G., and Gombos, G. (1981). Specific and artefactual cellular localizations of S 100 protein: an astrocyte marker in rat cerebellum. Dev. Neurosci. *4*, 66–78.
31. Pringle, N.P., and Richardson, W.D. (1993). A singularity of PDGF alpha-receptor expression in the dorsoventral axis of the neural tube may define the origin of the oligodendrocyte lineage. Development *117*, 525–533.
32. Ono, K., Yasui, Y., Rutishauser, U., and Miller, R. (1997). Focal ventricular origin and migration of oligodendrocyte precursors into the chick optic nerve. Neuron *19*, 283–292.
33. Spassky, N., Goujet-Zalc, C., Parmantier, E., Olivier, C., Martinez, S., Ivanova, A., Ikenaka, K., Macklin, W., Cerruti, I., Zalc, B., et al. (1998). Multiple restricted origin of oligodendrocytes. J. Neurosci. *18*, 8331–8343.
34. Zhou, Q., and Anderson, D.J. (2002). The bHLH transcription factors OLIG2 and OLIG1 couple neuronal and glial subtype specification. Cell *109*, 61–73.
35. Lu, Q.R., Sun, T., Zhu, Z., Ma, N., Garcia, M., Stiles, C.D., and Rowitch, D.H. (2002). Common developmental requirement for Olig function indicates a motor neuron/oligodendrocyte connection. Cell *109*, 75–86.
36. Spassky, N., Olivier, C., Perez-Villegas, E., Goujet-Zalc, C., Martinez, S., Thomas, J., and Zalc, B. (2000). Single or multiple oligodendroglial lineages: a controversy. Glia *29*, 143–148.
37. Fruttiger, M., Karlsson, L., Hall, A.C., Abramsson, A., Calver, A.R., Bostrom, H., Willetts, K., Bertold, C.H., Heath, J.K., Betsholtz, C., et al. (1999). Defective oligodendrocyte development and severe hypomyelination in PDGF-A knockout mice. Development *126*, 457–467.
38. Littlewood, T.D., Hancock, D.C., Danielian, P.S., Parker, M.G., and Evan, G.I. (1995). A modified oestrogen receptor ligand-binding domain as an improved switch for the regulation of heterologous proteins. Nucleic Acids Res. *23*, 1686–1690.
39. Yagi, T., Tokunaga, T., Furuta, Y., Nada, S., Yoshida, M., Tsukada, T., Saga, Y., Takeda, N., Ikawa, Y., and Aizawa, S. (1993). A novel ES cell line, TT2, with high germline-differentiating potency. Anal. Biochem. *21*, 70–76.
40. Dodd, J., Morton, S.B., Karagogeos, D., Yamamoto, M., and Jessell, T.M. (1988). Spatial regulation of axonal glycoprotein expression on subsets of embryonic spinal neurons. Neuron *1*, 105–116.
41. Helms, A.W., and Johnson, J.E. (1998). Progenitors of dorsal commissural interneurons are defined by MATH1 expression. Development *125*, 919–928.
42. Bermingham, N.A., Hassan, B.A., Wang, V.Y., Fernandez, M., Banfi, S., Bellen, H.J., Fritzsch, B., and Zoghbi, H.Y. (2001). Proprioceptor pathway development is dependent on Math1. Neuron *30*, 411–422.